Journal of Thermal Analysis and Calorimetry, Vol. 66 (2001) 179–195

A DSC STUDY OF HYDRATED SUGAR ALCOHOLS Isomalt

B. Borde and A. Cesàro*

Dep. of Biochemistry, Biophysics and Macromolecular Chemistry, University of Trieste, Via Giorgeri 1, I-34127 Trieste, Italy

Abstract

A DSC study has been carried out on isomalt, a commercial sugar alcohol derived from sucrose and widely used as a sweetener in the food industry. Isomalt is a mixture of two isomers: α-*D*-glucopyranosyl–1-6-mannitol (GPM) and α-*D*-glucopyranosyl–1-6-sorbitol (GPS). Release of the water of crystallisation (around 100°C) and melting (around 150°C) have been phenomenologically characterised using different scanning rates and heat treatments. The effect of dehydration/re-hydration on the melting has been investigated. The isomalt glass transition, at about 60°C, was studied on samples cooled after melting. The dynamic aspect of structural relaxation of isomalt has been quantified by its fragility parameter. Glassy state stability has been evaluated by performing ageing experiments at sub-T_g temperatures. During ageing, apart from the expected enthalpy relaxation effects, isomalt showed a peculiar behaviour, due to its isomeric composition. These preliminary and phenomenological results have been interpreted in terms of isomer structure and of carbohydrate-water interactions in the mixture.

Keywords: dehydration, DSC, isomalt, melting, structural relaxation

Introduction

Isomalt is a sugar alcohol appreciated in the food industry for its advantages in terms of sweetness, low-calorie content and non-cariogenicity. It is obtained from sucrose in a two-step process. Sucrose is first enzymatically converted to isomaltulose by changing the disaccharide bond from 1–2 to 1–6. Then, hydrogenation of isomaltulose (in aqueous solution with Raney nickel as catalyst) yields isomalt, an approximately equimolar mixture of α-*D*-glucopyranosyl–1-6-mannitol (GPM, Fig. 1a) and α-*D*-glucopyranosyl–1-6-sorbitol (GPS, Fig. 1b) [1, 2].

As shown in Figs 1a and b, the structural difference between GPM and GPS is confined to the carbon C–5 configuration of the acyclic polyol moiety. GPM crystallises as a di-hydrate: the two molecules of crystallisation water are fixed via hydrogen bonds to the mannitol portion, forming a 'double water bridge' between the oxygen atoms O–2 and O–5. In this structure, the mannitol portion is in a nearly pla-

* Author for correspondence, E-mail: borde@bbcm.univ.trieste.it

1418–2874/2001/ $ 5.00

Akadémiai Kiadó, Budapest
Kluwer Academic Publishers, Dordrecht

nar zigzag conformation [3]. Crystalline GPS is reported to be anhydrous, with its sorbitol portion in a non-linear bent-chain arrangement (as is *D*-sorbitol) [4].

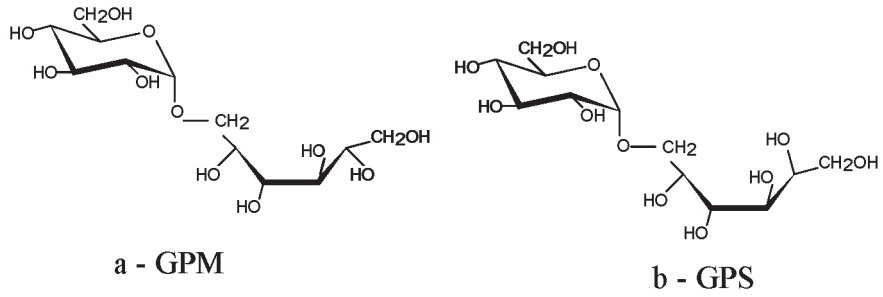

Fig. 1 Structure of the two isomeric components of isomalt

Isomalt is obtained as a crystalline material that melts around 142–150°C [1, 5], and after cooling gives a glassy state with a glass transition temperature at about 60°C [5–7] (also example in Table 1). As pure materials, GPM and GPS have quite similar thermodynamic properties (Table 1). Considering isomalt, an equimolar mixture of these two isomers, significantly lower melting temperatures and enthalpies are observed. This depression can be explained by the formation of a simple eutectic between the two sugar alcohols in the presence of water (two molecules per mole of GPM) [6]. The glass transition temperature value of isomalt appears to be intermediate.

Table 1 Melting and glass transition data of isomalt, GPS, GPM and the related alditols

Sample	T_{fus}/°C	$\Delta_{fus}H$/J g^{-1}	$\Delta_{fus}S$/J g^{-1} K^{-1}	T_g/°C	ΔC_p/J g^{-1} K^{-1}
Isomalt[a]	142	135	0.32	56.3	–
GPS[a]	166	163	0.37	50.5	–
GPM[a]	168	159	0.36	65.5	–
Sorbitol[b]	101.7	173.4	0.46	–1.3	1.24
Mannitol[b]	169.0	325.5	0.74	14.5	1.23

[a]Data from [6]. Crystalline samples were studied after drying for 1 h at 105°C (Q_h=5 K min^{-1}). For amorphous samples, Q_h=10 K min^{-1} and T_g's are fictive temperatures
[b]Data from [9]. For all samples, Q_h=2 K min^{-1}. Amorphous samples were quenched in liquid nitrogen

As a premiss to this study of isomalt, it is of interest to consider the properties of sorbitol and mannitol, the alditols corresponding to the acyclic moiety of GPS and GPM respectively. The correlation between the chain conformation of sorbitol and mannitol and their respective physical properties may indeed be relevant also for their sugar alditols. Molecular dynamics studies have assessed that the almost planar zigzag conformation of sorbitol obtained for 'in vacuo' simulations becomes bent in aqueous solution because of the interactions with water. More generally, this study has confirmed that the respective configurations of sorbitol and mannitol are determined by solute-solvent interactions [8].

Sorbitol and mannitol do not have the same solubility in water [2]. This discrepancy is attributed to different packing energies in their crystalline state: the melting temperature, enthalpy and entropy changes are indeed higher for mannitol than for sorbitol (Table 1). Although GPM and GPS differ also in their solubility, with values approaching those of their respective alditols [2], their melting points are very similar and nearly equal to that of mannitol (168 and 166°C respectively). The entropy changes associated with the melting of GPM and GPS are significantly lower than for their alditols, 0.36 and 0.37 J g^{-1} K^{-1} respectively. Glass transition temperatures and heat capacity increments ΔC_p are –1.3°C and 1.24 J g^{-1} K^{-1} for sorbitol and 14.5°C and 1.23 J g^{-1} K^{-1} for mannitol respectively. For their corresponding sugar alditols, the trend T_g sorbitol < T_g mannitol is conserved, but the glass transition temperatures are significantly higher (50.5°C for GPS and 65.5°C for GPM), as a consequence of higher molecular masses.

In order to gain a better understanding of the behaviour of isomalt, thermal properties of both its crystalline and amorphous states have been investigated by DSC. Focusing on the commercial products and industrial preparations, release of the water of crystallisation and melting of the eutectic mixture were characterised using different scanning rates and heat treatments. Like other carbohydrates used in food or confectionery products, isomalt is very often employed in its amorphous form. The study of this out-of-equilibrium physical state is of great relevance when considering not only the material properties during processing, but also its final quality. The stability of isomalt during storage at sub-T_g temperatures has been investigated and the rate of transformability with the temperature at T_g has been quantified by its fragility parameter [10, 11].

Experimental

Materials

Isomalt (Palatinit® produced by Sudzuecker AG-Mannheim/Ochsenfurt) was a commercial sample, kindly provided by Khan. The sample, received as white crystalline grains (typically 2 mm in diameter), was reduced to a powder by gentle hand grinding in a mortar. GPS, labelled as isomaltitol, α-*D*-glucopyranosyl–1-6-glucitol (glucitol is a synonym of sorbitol) was obtained from Sigma and used as received. The isomer composition of isomalt was established by high-performance anion-exchange chromatography (HPAEC)-pulsed amperometric detection (PAD) [12, 13]. Chromatographic separation of the two isomers and comparison with pure GPS revealed 45% of this component in the mixture.

Calorimetric measurements

All calorimetric measurements were carried out by using a Perkin Elmer DSC6. Temperature and heat flow were periodically calibrated with indium and tin standards using a heating rate Q_h=10 K min^{-1}. Samples of 5 to 10 mg were sealed in aluminium

pans: a hole made with a syringe needle in the pan cover allowed free water evaporation during measurements. Baselines were recorded for each set of measurements, and automatically subtracted from the total heat flow.

In the dehydration and melting experiments, the first scan of each sample was performed at Q_h ranging from 0.3 to 30 K min^{-1} and subsequent cooling ramps were systematically controlled, using a standard cooling rate Q_c of 10 K min^{-1}. Calibration with indium showed an instrumental deviation inferior to 1 K in the range of scanning rates explored here. Because of the large variation in the shape of the observed peaks, all transitions were identified by the peak temperature rather than with T_{onset}. Experiments including short isotherms for dehydration were performed in the calorimeter: samples were heated from 20°C to the desired temperature with Q_h=10 K min^{-1}, held at that temperature for the chosen time and then cooled with Q_c=10 K min^{-1}.

Glass transitions were studied by scanning amorphous samples between 10 and 120°C with Q_h=10 K min^{-1}. For the determination of the fragility parameter, cooling rates ranging from 0.1 to 10 K min^{-1} were used: the same sample was submitted to all thermal cycles without being removed from the calorimeter. Fictive temperatures, T_{fict}, were determined upon a subsequent heating scan at 10 K min^{-1}, following the procedure given in the literature [14]. Amorphous samples were studied after ageing at 20 or 30°C for times ranging from 1 to 35 days. These samples were immediately sealed in DSC pans after melting and cooling, and stored at constant temperature.

Heat capacity increment at the glass transition, ΔC_p, was taken at the middle of the transition. The parameters T_{fict}, ΔC_p and the enthalpy changes ΔH (for dehydration and melting transitions) were calculated using the Pyris Software by Perkin Elmer. The uncertainty was typically of the order of (or less than) 0.4°C for temperatures and 4% for enthalpy changes. The quantities ΔC_p and ΔH were expressed per gram of initial product, unless otherwise specified.

Results and discussion

Phase transitions in crystalline isomalt

Preliminary characterisation

A typical curve recorded for crystalline ground isomalt from 20 to 180°C (heating rate, Q_h=10 K min^{-1}) is shown in Fig. 2. The endothermic peak in the region 65–120°C was attributed to a progressive dehydration, as was shown by independent mass loss determination. The dehydration process exhibits a shoulder followed by a maximum at 97°C, a value of 71 J g^{-1} is measured for the vaporisation enthalpy $\Delta_{vap}H$ (Fig. 2). Very scarce data are found in literature about the endotherm associated with water removal from the crystalline form of isomalt. Commercial isomalt is reported to contain approximately 5–7% (mass/mass) of water [1]. Since an amount of 9.47% of water is theoretically associated with pure crystalline GPM, our commercial preparation of isomalt should contain about 5.2% of crystallisation water (GPM mass fraction is 0.55).

Melting of isomalt occurs broadly at higher temperatures, typically from 130 to 160°C. For the example shown in Fig. 2 the temperature (peak) of fusion, T_{fus}, and the fusion enthalpy changes, $\Delta_{fus}H$, are 150°C and 115 J g^{-1}, respectively. These results roughly compare with literature data ([1, 6] and Table 1 – Different measurement conditions).

Influence of grinding and humidity

Preliminary experiments showed that the grinding of the isomalt grains provided more reproducible DSC traces, mainly because thermal contact was improved. However, it is known that grinding affects the surface behaviour of the material. Using a slow heating rate (Q_h=3 K min^{-1}), the dehydration process shows two distinct events for both samples of isomalt, either as-received or ground as illustrated in Fig. 3 (curves 1 and 2). Grinding modifies the shape of the dehydration peak, giving a better-resolved low temperature shoulder and a smoother peak in the high temperature region. A return to the baseline is observed after dehydration for the ground sample whereas for the as-received sample, dehydration and melting are less clearly separated. The melting endotherm of the ground sample indeed starts at a higher temperature and does not present the low temperature shoulder observed for the as-received sample. The value of $\Delta_{fus}H$ for the freshly ground sample is reported in Table 2 together with other data, 42.8 kJ mol^{-1} (dry basis), while the literature gives 46.5 kJ mol^{-1} [6]. Before commenting on this difference, we shall report on other phenomenological observations about the effect of humidity and dehydration on melting.

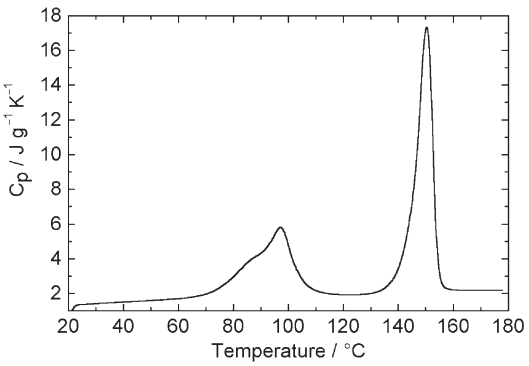

Fig. 2 Typical curve obtained for crystalline ground isomalt (Q_h=10 K min^{-1})

In addition to the above-mentioned changes, after grinding, isomalt becomes sensitive to the surrounding humidity. Figure 3 compares the curves obtained for isomalt immediately after grinding (curve 2) and after equilibration for four months at room humidity (relative humidity RH~50% – curve 3) or over a saturated NaCl aqueous solution at 20°C (RH 75% – curve 4). When exposed to external humidity, freshly ground isomalt easily takes in additional water. This is shown by the increase

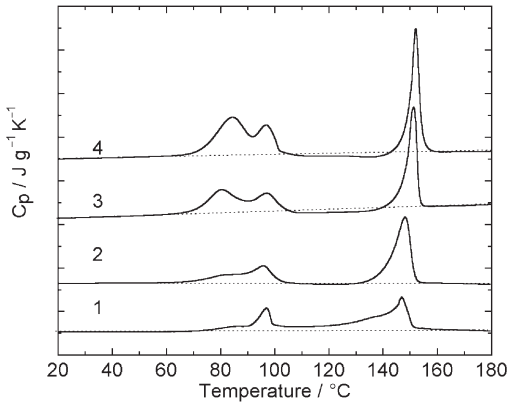

Fig. 3 Effect of grinding and humidity on isomalt C_p curves (Q_h=3 K min^{-1})
1 – as received sample; 2 – freshly ground sample; 3 – equilibrated at room humidity; 4 – equilibrated over NaCl saturated solution at 22°C (curves have been shifted for sake of clarity)

in the low-temperature endotherm related to water removal, the heat of vaporisation varying from 70 to 178 J g^{-1} (Table 2). Melting peaks are also slightly modified: they become thinner and are shifted towards high temperatures upon increasing moisture. The measured heat of fusion significantly increases after exposure to NaCl saturated solution (the enthalpy changes expressed in kJ per mole of anhydrous isomalt in Table 2). This effect could be associated with partial re-crystallisation during heating as indicated by the broad exothermic effect observed before melting (Fig. 3, curve 4).

Table 2 Heat of vaporisation and fusion measured for isomalt after different thermal and rehydration treatments

Sample	$\Delta_{vap}H$/J g^{-1}	Water content[a]/%	$\Delta_{fus}H^b$/ J g^{-1}	$\Delta_{fus}H^c$/ kJ mol^{-1}
Freshly ground	70	5	118	42.8
Room humidity	121	9	111	42.0
NaCl	178	13	125	49.6
5 h at 60°C	84	6	115	42.2
½ h at 80°C	49	4	117	42.0
1 h at 80°C	35	3	121	42.7
1 h at 90°C	2	<1	118	40.9
1 h at 105°C	0	0	123	42.3
1 h at 105°C+2 days over NaCl	119	9	70	26.4
1 h at 105°C+50 days over NaCl	123	9	52	19.7

[a]Evaluated from the $\Delta_{vap}H$ values with the hypothesis of the theoretical 5.2% H_2O for the freshly ground sample
[b]Per gram of initial product, i.e. partially to fully dried
[c]Per mole of anhydrous isomalt (M_w=344.32 g)

Influence of heating rates on the thermal behaviour

Freshly ground isomalt samples have been studied by using DSC heating ramps from 20 to 180°C, with Q_h spanning from 0.3 to 30 K min^{-1}. Upon decreasing heating rates (Fig. 4), the removal of water from the crystalline form is shifted to lower temperatures. For instance, the beginning of the dehydration process moves from 72°C for Q_h=10 K min^{-1} to 55°C for Q_h=0.3 K min^{-1}. Furthermore, two distinct events appear in the evaporation endothermic process.

Similarly, the shape of the melting peak changes as a function of the heating rate. For low heating rates, up to 1 K min^{-1}, a marked asymmetry is shown with a large pre-melting region. Higher heating rates (3 K min^{-1} or more) induce a small shift of the melting peak towards high temperatures and reduce the pre-melting exothermic effects. While some of these effects could be ascribed to the well-known behaviour of curve shapes upon changes of scanning rates, several comments will be necessary as long as these results may also depend on structural transformations in the sample. Melting enthalpies (taken from curves of Fig. 4) are reported in Fig. 5 as a function of the heating rate. $\Delta_{fus}H$ values show a dependence on the scanning rate with a small plateau (about 115 J g^{-1}) in the middle range of Q_h, whereas variations higher than the experimental error (about 4%) are observed at lower or higher heating rates. The increase of melting enthalpy at lower scanning rates can be ascribed to the underlying cold crystallisation in the range of 100–120°C, shown by the broad exothermic effects before melting. This observation may also explain the different shapes of the melting peaks.

Dehydration of isomalt

Ground isomalt samples equilibrated at room humidity were submitted to various heat treatments in order to understand the underlying process associated with the double peaks observed during dehydration. In a first experiment, isomalt was subjected to a short thermal cycle including heating and subsequent cooling between 20 and 120°C (Q_h=3 K min^{-1}, Q_c=10 K min^{-1}). A curve of this fully dehydrated sample was then recorded between 20 and 180°C (Fig. 6, curve 1). In place of the wide vaporisation endotherm, a small step is observed with a mid-point at 63°C and a C_p increment of 0.15 J g^{-1} K^{-1}, the rest of the curve showing a melting peak similar to that of an untreated sample. The similarity of the melting peaks is not surprising since these samples do not significantly differ in their structures immediately before melting. The assignation of the C_p step to a glass transition is spontaneous and may be explained in different ways. Around 5% of the water present in isomalt is intrinsic to the crystalline structure: amorphisation caused by the dehydration process is therefore highly probable as was, for instance, observed for raffinose [15]. The pre-existence of a small amorphous phase in our ground hydrated sample cannot be excluded either, the glass transition being possibly hidden by the vaporisation endotherm (Fig. 4, same Q_h, 3 K min^{-1}). Our commercial product may not be fully crystalline, as was reported for isomalt in other studies (88% of crystalline phase in [16]) and our hand grinding (though gentle) may have destabilised part of the crystalline structure.

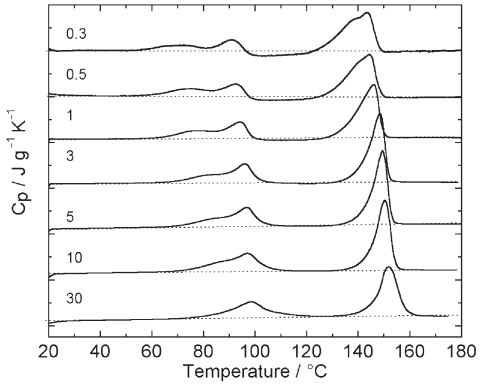

Fig. 4 C_p curves recorded for ground isomalt at different heating rates (Q_h are indicated in K min^{-1} on each curve. Curves have been shifted for sake of clarity)

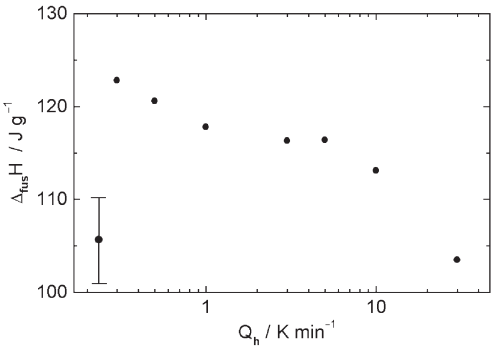

Fig. 5 Melting enthalpies of freshly ground isomalt as a function of the heating rate. (The 4% error bar is shown)

Comparing the measured ΔC_p value (0.15 J g^{-1} K^{-1}) with the ΔC_p obtained for a fully amorphous isomalt (0.80 J g^{-1} K^{-1} as will be seen in more detail in the following part and Fig. 8), one may infer that around 19% of the sample is amorphous after dehydration. This evaluation can only be approximate since the real ΔC_p of the amorphous material observed after dehydration may differ from ΔC_p of bulk isomalt. The difference in ΔC_p may stem from a difference in composition since the new amorphous phase may reasonably contain more GPM (crystallised as di-hydrate, unknown ΔC_p) than GPS (ΔC_p measured in the same conditions as for isomalt=0.90 J g^{-1} K^{-1}). A depression of ΔC_p is also reported for the 'rigid amorphous' phase [17], the molecular mobility being reduced when the material is constrained by the presence of crystallites.

For a better insight into the phenomenon, partial dehydration experiments were also carried out. In this case, isothermal stages were chosen rather than further dynamic experiments. Several samples were kept isothermally at 60°C (5 h), 80°C (0.5 and 1 h), 90°C (1 h) and 105°C (1 h), thus undergoing a partial-to-complete dehydration as confirmed by the decrease in the corresponding endotherms in Fig. 6 (curves

2–6 respectively and data in Table 2). The different treatments first affect the low-temperature dehydration peak and finally the high-temperature dehydration peak. The mild drying at 60°C does not modify the shape of the dehydration peaks while after 1 h at 80°C only an almost symmetric dehydration peak at higher temperatures remains (curves 2 and 4). For all samples subjected to drying treatments up to 90°C, a small step is observed in the C_p curve. Very similar to the glass transition that was observed after heating to 120°C, it is characterised by a mid-step temperature at around 64°C and a small maximum at 67°C (insert, Fig. 6).

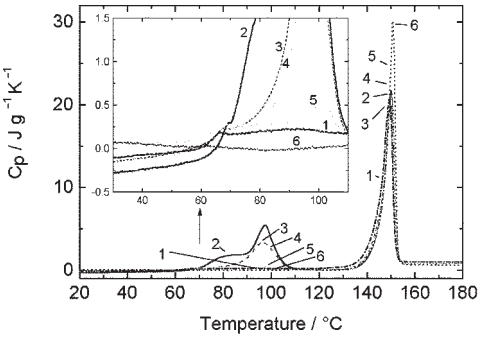

Fig. 6 C_p curves of isomalt after various dehydration treatments (Q_h=3 K min^{-1})
1 – scan from 20 to 120°C; 2 – 5 h at 60°C; 3 – ½ h at 80°C; 4 – 1 h at 80°C;
5 – 1 h at 90°C; 6 – 1 h at 105°C

The constant position of the step for all samples may be quite puzzling. It indicates that the amorphous phase progressively formed during dehydration is neither sensitive to the residual water content nor influenced by the structural state of the surrounding micro-structured components. An explanation for these observations is the progressive formation of the amorphous phase (anhydrous) by dehydration of the crystalline structure. The newly formed amorphous zones are thus distributed among other micro-structured hydrated phases and poorly influenced by the overall water content (mainly crystallisation water).

The absence of a C_p step in the curve recorded for the sample dried at 105°C is less surprising as it is typical of an amorphous re-crystallisable phase sufficiently cured above its glass transition temperature. A slight structural reorganisation takes place in all of the (partially to fully) dehydrated samples. Upon completing the removal of water from crystalline isomalt, melting peaks indeed show greater amplitude and are slightly shifted towards higher temperatures. Coinciding with these observations, the measured enthalpy slightly increases from 111 (hydrated sample) to 123 J g^{-1} (fully dehydrated sample) (Table 2). However, the intermediate values have to be considered carefully as they refer to samples with variable water contents. The occurrence of a variable amount of amorphous phase formed during dehydration makes the evaluation of the enthalpy of fusion difficult while the vicinity of T_g step and water removal endotherm renders the evaluation of the heat of vaporisation imprecise. A high extent of amorphisation by removal of the

crystallisation water may explain the very low value obtained for the $\Delta_{fus}H$ after treatment at 90°C whereas partial re-crystallisation may account for the higher melting enthalpy measured after 1 h at 105°C.

Confirmation and analysis of the origin of all these observations require other kinds of investigations based on structural (X-rays) and dynamical (TM-DSC) methods.

Re-hydration of isomalt

In order to check the stability of dried isomalt towards external humidity, samples were submitted to complete drying and further exposed to water vapour. A drying of 1 h at 105°C was applied to isomalt powder placed in open DSC pans in an oven. As has been previously shown, this thermal treatment induces a complete dehydration of isomalt and allows improvements in the crystalline structure, sufficient to cancel the previous glass transition. The dried samples were then stored for re-hydration for 2 and 50 days at 20°C over a saturated NaCl aqueous solution and finally submitted to a DSC heating scan. The corresponding curves (curves 3 and 4 in Fig. 7) are compared with those of a sample scanned immediately after the dehydration process (curve 2) and of an untreated hydrated sample (curve 1). For dried isomalt, the progressive uptake of water leads to the formation of a hydrated state that loses water at a high temperature (around 100°C). Quite surprisingly, the amount of added water is already high after 2 days over NaCl saturated solution and does not significantly increase during further storage (Table 2).

Scrutinising the de-hydration peak and the fusion enthalpy changes makes the effect of hydration water on the melting clear. With a scan rate of 3 K min^{-1}, a broad melting peak with an enthalpy change of 118 J g^{-1} is observed for the untreated sample, while a slightly larger value (123 J g^{-1}) and a sharper peak is shown by the fully dried sample (Fig. 7). After water uptake, the dried sample shows a significantly reduced melting peak: its melting enthalpy is lowered to 52 J g^{-1} (corresponding to 19.7 kJ mol^{-1}), after a storage of 50 days at 75% of relative humidity (Fig. 7 and Ta-

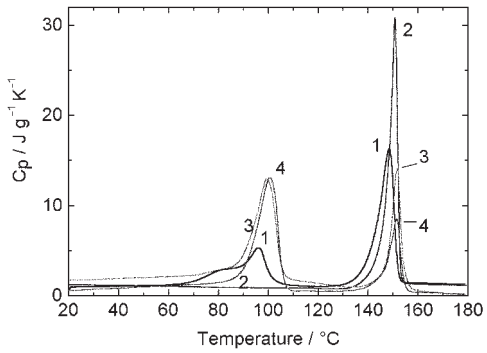

Fig. 7 C_p curves of isomalt after various dehydration/re-hydration treatments (Q_h=3 K min^{-1}). 1 – untreated sample, 2 – dried in oven for 1 h at 105°C; 3 – dried in oven for 1 h at 105°C and stored for 2 days over NaCl saturated solution at 22°C; 4 – dried in oven for 1 h at 105°C and stored for 50 days over NaCl saturated solution at 22°C

ble 2). This peak remains sharp and is shifted to a higher temperature with respect to the dried sample.

From the high temperature position of the dehydration peaks in Fig. 7 (curves 3 and 4), it is inferred that water molecules are tightly bound to some sugar molecules. The additional water taken by these samples during re-hydration can be found in various locations: adsorbed on the crystal surface, inserted in new crystalline structures or absorbed by an amorphous phase, undetected by DSC. In all cases, the decrease in the final melting peak indicates the development of a new phase at the expense of eutectic crystals. This phase can be hypothesised as a new hydrated crystalline form (melting around 100°C) or as the result of a progressive amorphisation of the material.

Independently of any hypothesis, these observations indicate that, even if the amount of crystalline structure of isomalt mixture may be slightly increased by annealing at 105°C, the two components are necessarily nano-structured and water sensitive. After complete water removal, the resulting composite is 'unstable' in the sense that it can be destroyed (at least partially) if exposed to humidity. The presence of nano-structured crystals (like para-crystalline material) is corroborated by the literature observation that the 'amounts of amorphous isomalt from experimental solution enthalpies do not agree with those provided by X-ray powder diffraction studies' [16].

Isomalt/water interactions

Slow heating rates have revealed a bimodal dehydration process in ground crystalline isomalt. The presence of 55% of GPM di-hydrate in the crystalline mixture may give the most obvious explanation for this two-step dehydration process. Two structurally different water molecules are present in the GPM crystal and therefore leave the solid at different times/temperatures. However, the presence of water out of the GPM domains of isomalt cannot be excluded. Although our ground samples did not show any glass transition on first DSC scans, their non-complete crystallinity can also be invoked: amorphous phases are more hygroscopic than crystals. Furthermore, the eutectic mixture forming isomalt may give a different molecular behaviour with respect to pure GPM and GPS. While GPS has been reported as an anhydrous crystal only, the formation of several polymorphs of sorbitol has been known for a long time [18]. This peculiarity suggests the presence of water in contact with GPS molecules in addition to the expected distribution within the GPM fraction.

Small and broad exothermic effects before melting and slight modifications of the melting peaks (increase in area, temperature position, and amplitude) have been observed for low heating rates or for highly hydrated samples (Figs 3 and 4). Heat treatments at 105°C led to similar changes. Cold crystallisation is made possible by thermally favoured molecular mobility, and seems also to be enhanced in the case of higher initial water contents. Although these rearrangements occur at high temperatures after dehydration, both GPM and GPS may be involved: in the nano-structured composite resulting from dehydration, anhydrous GPM must be particularly unstable and thus likely to form more favourable structures, even with GPS.

Glassy isomalt and structural relaxation

Glass transition

While many small molecules re-crystallise easily on cooling after a complete melting, isomalt may be cooled with a Q_c as slow as 0.3 K min^{-1} without any re-crystallisation, as was observed for sugars like trehalose [19]. A typical curve obtained for amorphous isomalt (anhydrous) prepared with Q_c=10 K min^{-1} and registered at the same heating rate is presented in Fig. 8. The characteristic parameters are T_{fict}=60°C and ΔC_p=0.80 J g^{-1} K^{-1}. The glass transition is marked by some enthalpy relaxation effects giving a peak maximum at 65.8°C. These results agree fairly well with data taken from literature [6], although it should be mentioned that the glass transition temperature and fictive temperature depend on the cooling rate, a parameter that is rarely mentioned in literature. In the following, a characterisation of various aspects of structural relaxation in isomalt is given, with particular attention to thermal histories.

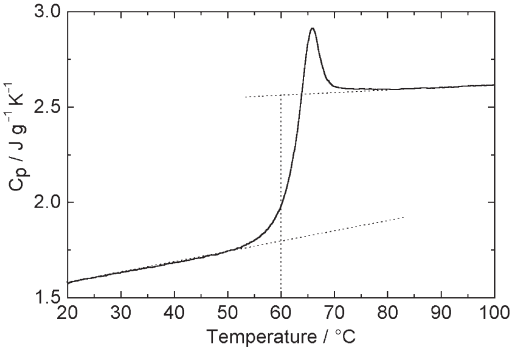

Fig. 8 Typical C_p curve obtained for amorphous isomalt (Q_c=Q_h=10 K min^{-1})

Isomalt fragility parameter

The fragility parameter, *m*, has been devised as a distinctive property that characterises dynamic relaxation at molecular level in glass forming liquids [10, 11], and in practice is quantified by the dependence of relaxation times on temperature changes in the region approaching the glass transition. For fragile liquids this derivative (i.e. the activation energy) is definitely larger than for strong liquids.

The fragility parameter has been originally defined for physical properties associated with segmental relaxation dynamics (e.g. viscosity) and evaluated from the relaxation time τ, plotted as a function of reciprocal temperature, scaled by a reference temperature (commonly the glass transition temperature), namely T_g/T [10]:

$$m=\left.\frac{\mathrm{d}\log_{10}(\tau)}{\mathrm{d}\frac{T_g}{T}}\right|_{T=T_g}$$

A parameter m_h (conceptually similar but not necessarily equal to m) can be determined by calorimetric measurements, from the cooling rate dependence of the glassy fictive temperature T_{fict}, by using a method described by Moynihan *et al.* [14] and summarised in the following equations:

$$\frac{\mathrm{d}\ln|Q|_c}{\mathrm{d}\left(\frac{1}{T_{fict}}\right)} = -\frac{\Delta H^*}{R} \text{ and thus } m_h = \frac{\Delta H^*}{2.303RT_g}$$

ΔH^* is the activation energy used in several models for the simulation of enthalpy relaxation, and R is the gas constant. For the reference temperature T_g, the value of the fictive temperature of a standard glass obtained with Q_c=Q_h=10 K min^{-1} was used.

The fragility parameter m_h of isomalt has been evaluated by measuring the fictive temperatures of glasses obtained after cooling with Q_c spanning from 0.1 to 30 K min^{-1} (curves are reported in Fig. 9). From the data of ln(Q_c) as a function of the reciprocal fictive temperature of the various glasses (Fig. 10), the values 897±50 and 140±8 kJ mol^{-1} have been evaluated for the apparent activation energy ΔH^* and the fragility parameter m_h, respectively. With a m_h value higher than 100, isomalt fits within the class of fragile liquids in the strong/fragile classification [10].

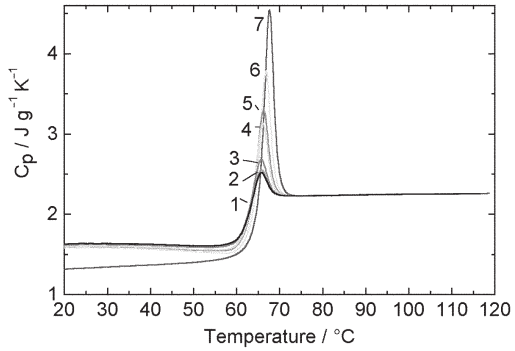

Fig. 9 C_p curves of amorphous isomalt recorded after different cooling rates Q_c (Q_h=10 K min^{-1}). 1 – Q_c=10 K min^{-1}; 2 – Q_c=8 K min^{-1}; 3 – Q_c=4 K min^{-1}; 4 – Q_c=1 K min^{-1}; 5 – Q_c=0.7 K min^{-1}; 6 – Q_c=0.3 K min^{-1}; 7 – Q_c=0.1 K min^{-1}

Concerning the general aspect of the curves of Fig. 9, an increasing enthalpy relaxation peak is observed by decreasing cooling rates. The peaks with increasing amplitude are also slightly shifted towards higher temperatures, as generally described for glassy materials, from small molecules to high molecular mass polymers [20]. Whereas all curves coincide perfectly in the high temperature region of the undercooled liquid state, the glassy heat capacity values appear to be somewhat dependent on the previous cooling rate. This effect may be related to the small size of our experimental window: real glassy heat capacity may not depend on the cooling rate but C_p may be affected by some relaxation effects during heating, before the main glass tran-

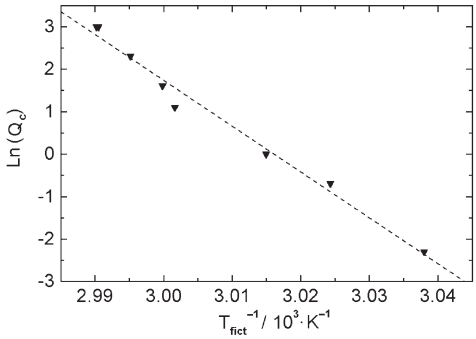

Fig. 10 Arrhenius plot for the calculation of the fragility parameter m_h (T_{fict} values from Fig. 9)

sition. A large distribution of relaxation times associated with the glass transition can easily account for this behaviour. Whether the further difference observed for Q_c=0.1 K min^{-1} (double experiment) is due to measurement or instrumental artefact is to be ascertained, as it is outside of this progressive change.

Physical ageing of glassy isomalt

Ageing experiments have been performed at 30, and at 20°C, for times t_a comprised between 1 and 35 days. In order to avoid possible complications associated with water absorption, these experiments were carried out in sealed pans. The DSC curves of the samples aged at 30°C (Q_h=10 K min^{-1}) are reported in Fig. 11. In addition to the increasing enthalpy relaxation effects on the 'main' glass transition at 66°C, a step is already observed on the glassy C_p at around 37°C only after two days of ageing. Upon increasing ageing time, this step is shifted towards higher temperatures and develops into a peak similar to the one observed at the glass transition. Simultaneously, the

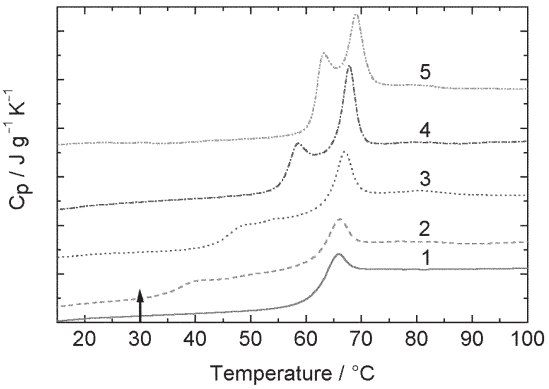

Fig. 11 C_p curves obtained for amorphous isomalt aged for various times at 30°C (Q_h=10 K min^{-1}). 1 – unaged sample; 2 – 2 days; 3 – 5 days; 4 – 14 days; 5 – 27 days (curves have been shifted for sake of clarity)

enthalpy recovery peak observed at the glass transition is slowly shifted towards higher temperatures and is enhanced with increasing t_a.

Lowering the ageing temperature to 20°C, the same effects are observed although to a lesser extent. The enthalpy relaxation peak around 66°C is less developed and moves only slightly towards high temperatures. A low temperature step appears also at lower temperatures (after two days, maximum at 36 rather than 40°C) and it moves slowly, without reaching the glass transition (at 50°C, after 35 days of ageing – Fig. 12, curves 1 to 6).

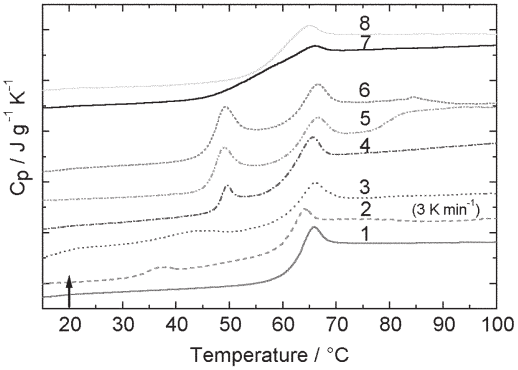

Fig. 12 C_p curves obtained for amorphous isomalt aged for various times at 20°C (Q_h=10 K min^{-1} except for curve 2). 1 – unaged; 2 – 2 days; 3 – 8 days; 4 – 13 days; 5 – 28 days; 6 – 35 days; 7 – second scan (120°C); 8 – second scan (180°C) (curves have been shifted for sake of clarity)

Considering the glass transition region only, our observations correspond to the typical behaviour of any glassy substance stored at temperatures below T_g. The development of the enthalpy relaxation peak (increase in amplitude and shift towards higher temperatures) classically depends both on ageing time and ageing temperature [20]. The simultaneous apparition of the second step/relaxation peak (showing also a regular evolution with time and temperature) in the low temperature part of the curves is more surprising. In the preceding study of glass transition and fragility, indeed isomalt behaved as a single component and showed a unique glass transition, indicating a perfect miscibility of GPM and GPS.

It is also interesting to note that the second scan of aged samples (cooled at 10 K min^{-1} after the heating scan from 10 to 120°C) does not show the same curve as the unaged samples (Fig. 12, curves 7 and 1). In curve 7, the glass transition appears spread over a wide range of temperatures, from 45 to 70°C. This discrepancy indicates that the thermal treatment up to T_g +60°C was not sufficient to erase completely the thermal history of the aged samples. Though still different, the second scan of a sample after heating to 180°C, is more similar to that observed for the unaged sample (Fig. 12, curves 8 and 1). This observation may indicate further modifications in the rubbery material, likely to cancel almost completely the thermal history of our samples.

Although unexpected, a kind of phase separation seems to occur during physical ageing of isomalt. At the beginning of ageing experiments, the new 'phase' shows a glass transition temperature significantly lower than those of GPM and GPS (T_{fict} given as 65.5 and 50.5°C respectively [5]). Increasing the ageing time shifts the position of the corresponding peak towards high temperature in such a rapid manner that a more drastic change must occur in addition to the classical effects of ageing. If a simple composition effect [21] can account for the intermediate value of the isomalt main glass transition temperature (T_{fict} given as 56.3°C measured in the same conditions as for GPM and GPS [5]), it cannot be responsible for such a high T_g depression in absence of any other component (water was removed during melting).

Dealing with isomalt, a mixture of isomers, the formation of micro-domains may be invoked rather than a pure phase separation. Local rearrangements of the initially randomly distributed isomers GPM and GPS and changes in the molecular conformations of their linear chains may allow peculiar packing in localised regions. In the initial phase of this evolution, because of their reduced size, these new domains may recover certain mobility very easily, thus showing a very low T_g. With the progressive generalisation of this process (and cancellation of the low size effect), their T_g may increase rapidly again, until reaching the T_g value corresponding to the bulk material. The necessity for a high temperature treatment to erase ageing effects in the material supports this hypothesis. The local rearrangements being more advanced than in the case of a simple ageing, their 'homogenisation' requires more energy. These interpretations remain in the field of speculations; further ageing experiments as well as structural techniques would be required for a more accurate characterisation of the evolution of the glassy isomalt structure.

Conclusions

In this study carried out in various conditions of temperature and humidity, the complex behaviour of isomalt has been widely characterised, in both crystalline and amorphous states. In the light of these experiments, various hypotheses have been formulated, either based on carbohydrate/water interaction or on the specificity of isomer configurations.

Dehydration/re-hydration experiments show a high non-reversibility with deep modification of the crystalline structure. Dehydration induces a partial amorphisation of the crystalline mixture: according to time and temperature conditions, this molecular mobility remains 'potentially active' in an amorphous phase or leads to improvements of the structural organisation during annealing or cold crystallisation. Freezing of molecular motions and reluctance to reversibility find correspondence with the character of fragile liquid exhibited by isomalt. These effects and the peculiar behaviour of isomalt aged at sub-T_g temperatures may be related to changes in conformations allowing a different packing in the amorphous phase.

Some of the present hypotheses demand further experiments for a definitive assessment. Structural investigation of the transformations occurring during the thermal treatments is necessary. These studies are in progress by means of powder X-ray

diffraction and will complete the preliminary thermal characterisation given here. Temperature modulated DSC measurements are also planned to provide more details on the water removal process and the simultaneous structural modifications of isomalt as well as on the dynamic aspect of the glass transition.

* * *

This research is supported by the University of Trieste and by a Marie Curie Fellowship of the European Community programme 'Improving Human Potential' under contract number HPMF-CT–1999-00166.

The authors thank Prof. T. R. I. Cataldi, Dr. M. Angelotti and Dr. C. Campa for the assessment of isomalt composition by HPAEC PAD.

References

1 H. Schiweck, Alimenta, 19 (1980) 5.
2 H. Schiweck, M. Munir, K. M. Rapp, B. Schneider and M. Vogel, Carbohydrates as Organic Raw Materials, F. W. Lichtenthaler, Weinheim 1991, p. 57.
3 H. J. Lindner and F. W. Lichtenthaler, Carbohydr. Res., 93 (1981) 135.
4 F. W. Lichtenthaler and H. J. Lindner, Liebigs Ann. Chem., (1981) 2372.
5 H. K. Cammenga and B. Zielasko, Thermochim. Acta, 271 (1996) 149.
6 H. K. Cammenga and B. Zielasko, Ber. Bunsenges. Phys. Chem., 100 (1996) 1607.
7 J. Raudonus, J. Bernard, H. JanBen, J. Kovalczyk and R. Carle, Food Res. Int., 33 (2000) 41.
8 J. R. Grigera, J. Chem. Soc., Faraday Trans. 1, 84 (1988) 2603.
9 M. Siniti, J. Carré, J. M. Létoffé, J. P. Bastide and P. Claudy, Thermochim. Acta, 224 (1993) 97.
10 C. A. Angell, J. Non-Cryst. Solids, 131–133 (1991) 13.
11 R. Böhmer, K. L. Ngai, C. A. Angell and D. J. Plazek, J. Chem. Phys., 99 (1993) 4201.
12 T. R. I. Cataldi, C. Campa, I. G. Casella and S. A. Bufo, J. Agric. Food Chem., 47 (1999) 157.
13 C. Corradini, G. Canali, E. Cogliandro and I. Nicoletti, J. Chromatogr. A, 791 (1997) 343.
14 C. T. Moynihan, A. J. Easteal, M. A. DeBolt and J. Tucker, J. Am. Ceram. Soc., 59 (1976) 12.
15 A. Saleki-Gerhardt, J. G. Stowell, S. R. Byrn and G. Zografi, J. Pharm. Sci., 84 (1995) 318.
16 H. K. Cammenga, L. O. Figura and B. Zielasko, J. Thermal Anal., 47 (1996) 427.
17 B. Wunderlich, Thermochim. Acta, 300 (1997) 43.
18 S. Quinquenet, C. Grabielle-Madelmont and M. Ollivon, J. Chem. Soc., Faraday Trans. 1, 84 (1988) 2609.
19 F. Sussich and A. Cesàro, J. Therm. Anal. Cal., 62 (2000) 757.
20 I. M. Hodge, J. Non-Cryst. Solids, 169 (1994) 211.
21 L. Finegold, F. Franks and R. H. M. Hatley, J. Chem. Soc., Faraday Trans. 1, 85 (1989) 2945.